Supporting Information

Miller et al. 10.1073/pnas.1204151109

SI Materials and Methods

Mouse Model of Allergen-Induced Asthma. The mouse model of acute OVA (1), and *Alternaria* (2) induced Th2 and eosinophilic airway inflammation has been described. Mice were killed 24 h after the final challenge. The right lung was snap frozen in liquid nitrogen for RNA isolation. The left lung was fixed with 4% paraformaldehyde for paraffin embedding and immunostaining. In selected experiments, to obtain pure populations of bronchial epithelial cells, we used a bronchial brushing technique described in this laboratory (2). More than 95% of cytospun cells from bronchial brushings have the ultrastructural appearance of ciliated airway epithelial cells, immunostain positive for the epithelial marker E-cadherin, and express the transcript signature that includes mucus genes (2). In selected experiments, purified populations of BAL macrophages (>98% purity) were obtained by adhesion by placing BAL cells in a 10-cm Petri dish in complete media for 4 h. All animal experimental protocols were approved by the University of California at San Diego Animal Subjects Committee.

Neutrophils and Eosinophils. Purified populations of peripheral blood neutrophils (>98% purity) were obtained by using a percoll density gradient as described (3). Eosinophils (> 97% purity) were generated from the bone marrow of C57/Bl6 mice cultured in media containing 100 ng/mL SCF and FLT3 ligand (PeproTech) with 10 ng/mL IL-5 (R&D Systems) as described (4).

Detection of ORMDL3 mRNA and ORMDL Protein in the Lung and Lung Cells. ***Quantitative PCR (qPCR).*** Total RNA was extracted with RNA-STAT60 (Tel-Test) and reverse transcribed with Oligo-dT and SuperScript II Kit (Invitrogen). qPCR was performed with TaqMan PCR Master Mix Kit and ORMDL1, ORMDL2, ORMDL3, and Serca2b primers (Applied Biosystems). The relative amounts of transcripts were normalized to those of housekeeping gene (GAPDH) mRNA and compared between the different genes by the ΔΔCt method (5).

Immunohistochemistry. To determine whether lung cells express ORMDL protein, in collaboration with Abnova, we generated a rabbit polyclonal Ab to ORMDL3. The ORMDL3 protein sequence (HTVKGTPFETPDQGKARLLTHWEQMDYGVQFT-AS) used to immunize rabbits was prepared by Abnova. In addition, we purchased a polyclonal rabbit anti-mouse ORMDL3 Ab from Abgent.

Immunoflurescence microscopy. Immunostaining was performed with primary antibodies including a polyclonal rabbit anti-ORMDL antibody, and/or a chicken anti-mouse calreticulin Ab (Abcam) singly and in combination. Tyramide Signal Amplification Kit 41 (Invitrogen) was used for fluorescent signal amplification with subsequent DAPI staining (Vector Laboratories) as described in this laboratory (6). Lung airways were visualized with a DM2500 microscope (Leica Microsystems).

Confocal microscopy. Confocal microscopy of immunofluorescence stained lung sections (anti-ORMDL and anti-calreticulin Ab) was performed with a Zeiss LSM confocal microscope. (Magnification: 100×.) Slides were analyzed by using Velocity 3D Image analysis.

FACS. Lung processing was performed as described (7). To obtain lung single-cell suspensions, lungs were minced and shaken in RPMI medium 1640 with 2 mg/mL collagenase and 1 mg/mL DNase I (Roche) for 25 min. Lung cells were isolated by using a 70-μm cell strainer and were incubated with a rat monoclonal antibody to CD16/CD32 (2.4G2) to block Fc receptors. Cells were then surface stained for 30 min with various combinations of anti-mouse PerCP-conjugated CD45 (ebioscience), rat anti-mouse APC-conjugated E-cadherin (R&D Systems), rat anti-mouse PE-conjugated Siglec-F (BD Pharmingen), hamster anti-mouse FITC-conjugated CD11c (BD Pharmingen), hamster anti-mouse APC-conjugated CD11c (eBioscience), and rat anti-mouse APC-conjugated GR-1 (eBioscience). APC-conjugated rat IgG2A isotype control was used for surface E-cadherin staining (R&D Systems). Epithelial cells were identified as the CD45-negative E-cadherin–positive population. Macrophages were identified as CD45-positive Siglec-F–positive CD11c-positive cells or CD45-positive CD11c-positive autofluorescent positive cells (7). Eosinophils were identified as CD45-positive Siglec-F–positive CD11c-negative cells and neutrophils identified as CD45-positive CD11c-negative GR-1–positive cells. After surface cell staining, lung cells were resuspended in fixation/permeabilization solution (BD Cytofix/Cytoperm kit; BD Biosciences) followed by incubation with a polyclonal rabbit anti-mouse ORMDL3 Ab (Abgent) or polyclonal rabbit Ab (GeneTex) for 30 min. Cells were then washed and incubated with either PE-conjugated F(ab′)2 donkey anti-rabbit IgG (eBioscience) or APC-conjugated anti-rabbit IgG (R&D Systems). Flow cytometry was performed with an Accuri C6 flow Cytometer (BD), and data was analyzed with FlowJo software (Tree Star).

Administration of Th2 Cytokines (IL-4, IL-13) or TNF to the Airway of WT Mice. Eight-wk-old WT C57BL/6 mice (n = 3 per group) were challenged intranasally with 0.6 μg of each individual cytokine (IL-4, IL-13, TNF-α, or PBS diluent control) (R&D Systems) as described in this laboratory (8). Twenty-four hours after each individual cytokine or diluent challenge, the mice were killed and the lungs were processed for immunohistology to detect ORMDL expression in airway epithelium. In addition, bronchial brushing epithelial cells were processed for qPCR.

WT and STAT6$^{-/-}$ Bone Marrow Chimeras. WT (CD45.1) and STAT6$^{-/-}$ (CD45.2) bone marrow chimeras were generated as described (2). Efficiency of chimerism was >95% as assessed by FACS for congenic markers CD45.1 and CD45.2 on BAL cells (2). Mice were rested for 6 wk before intranasal allergen challenge with *Alternaria* as described (2) and killed 24 h later at which timepoint lung specimens were processed for ORMDL immunostaining.

ORMDL Expression in Epithelial NF-κB–Deficient Mice. The lungs of *CC10*-Cre^{tg}/*Ikk*β$^{\Delta/\Delta}$–deficient mice (6) (unable to activate NF-κB in airway epithelium) and littermate controls were immunostained with an anti-ORMDL Ab to quantitate levels of ORMDL expression in airway epithelium by immunohistology and image analysis.

ORMDL Expression in Lung Smooth Muscle and Fibroblasts. The lungs of Col-1 GFP reporter mice, and α-smooth muscle actin RFP reporter mice (kindly provided by David Brenner, University of California, San Diego) (9), were immunostained with an anti-ORMDL Ab, to detect whether ORMDL was expressed in lung fibroblasts or smooth muscle cells.

Transfection of ORMDL3 in Airway Epithelial Cells in Vitro. Human primary bronchial epithelial cells (ScienCell) and human epithelial cell line A549 (ATCC) were transfected with an ORMDL3 plasmid (OriGene) by using TurboFectin 8.0 reagent (OriGene) according the manufacturer's instructions.

Activation of ATF6 Signaling Branch in ORMDL3 Transfected Airway Epithelial Cells. We investigated whether ORMDL3 transfection of lung epithelial cells (A549) induced activation of ATF6, Ire1, or

PERK UPR pathways. Activation of ATF6 was detected by using two alternate methods, namely (*i*) immunofluorescence microscopy to detect nuclear localization of ATF6 by using an ATF6 Ab (Imgenex)(10), and (*ii*) a UPR reporter assay containing the ER stress element from the BiP promoter fused to luciferase (11-13). Activation of Ire1 was detected by PCR because it removes the UPR intron from the unspliced form of XBP1 (XBP1u) to generate the spliced form of XBP1 (XBP1s) mRNA (11). Activation of PERK was assessed by increased levels of phospho-eIF2α by Western blot using antibody specific to the phosphorylated form of eIF2α (11). In all UPR experiments, thapsigargin (Tg), a known activator of the UPR, was used as a positive control. Effects on the UPR upon Tg treatment (200 nM in DMSO, for 1 h) were compared with ORMDL3 transfection alone with DMSO (ORMDL3), and empty plasmid (pCMV6) upon DMSO or Tg treatment as described (12). In addition to the empty plasmid as a negative control, we performed similar experiments with a GFP-tagged ER transmembrane protein Sec61α-GFP (14).

Transfection of ATF6α siRNA in Airway Epithelial Cells in Vitro. Human epithelial cell line A549 (ATCC) were transfected with either an ATF6α or negative siRNA (OriGene) by using Lipofectamine RNAiMAX reagent (Invitrogen) according the manufacturer's instructions. The decrease of ATF6α expression was confirmed by qPCR with human ATF6α primers (OriGene). SERCA 2b primers were purchased from OriGene.

Western Blots. Protein lysates (transient overexpression lysate for ORMDL1, ORMDL2, ORMDL3, or SERCA2b) were purchased from Origene. Protein was separated on a SDS/PAGE gel and transferred to a PVDF membrane. Membranes were blocked in 5% (wt/vol) milk in 1× Tris-buffered saline with Tween for 1 h and then incubated with primary antibody overnight at 4 °C. The antibodies used in this study were rabbit polyclonal anti-ORMDL3 (Abgent), mouse monoclonal anti-Serca2b (Abcam), and rabbit monoclonal anti-GAPDH (Genetex). For blocking experiments, ORMDL3 blocking peptide (Abgent) were incubated with anti-ORMDL3 AB for 1 h.

1. Cho JY, et al. (2004) Inhibition of airway remodeling in IL-5-deficient mice. *J Clin Invest* 113:551–560.
2. Doherty TA, et al. (2012) Alternaria induces STAT6-dependent acute airway eosinophilia and epithelial FIZZ1 expression that promotes airway fibrosis and epithelial thickness. *J Immunol* 188:2622–2629.
3. Luo Y, Dorf ME (2001) Isolation of mouse neutrophils. *Curr Protoc Immunol* 3:20.1–20.6.
4. Dyer KD, et al. (2008) Functionally competent eosinophils differentiated ex vivo in high purity from normal mouse bone marrow. *J Immunol* 181:4004–4009.
5. Livak KJ, Schmittgen TD (2001) Analysis of relative gene expression data using real-time quantitative PCR and the 2(-Delta Delta C(T)) Method. *Methods* 25:402–408.
6. Broide DH, et al. (2005) Allergen-induced peribronchial fibrosis and mucus production mediated by IkappaB kinase beta-dependent genes in airway epithelium. *Proc Natl Acad Sci USA* 102:17723–17728.
7. Doherty TA, et al. (2011) The tumor necrosis factor family member LIGHT is a target for asthmatic airway remodeling. *Nat Med* 17:596–603.
8. Cho JY, et al. (2010) Chronic OVA allergen challenged Siglec-F deficient mice have increased mucus, remodeling, and epithelial Siglec-F ligands which are up-regulated by IL-4 and IL-13. *Respir Res* 11:154.
9. Magness ST, Bataller R, Yang L, Brenner DA (2004) A dual reporter gene transgenic mouse demonstrates heterogeneity in hepatic fibrogenic cell populations. *Hepatology* 40:1151–1159.
10. Thomas M, et al. (2005) The unfolded protein response modulates toxicity of the expanded glutamine androgen receptor. *J Biol Chem* 280:21264–21271.
11. Babour A, Bicknell AA, Tourtellotte J, Niwa M (2010) A surveillance pathway monitors the fitness of the endoplasmic reticulum to control its inheritance. *Cell* 142:256–269.
12. DuRose JB, Tam AB, Niwa M (2006) Intrinsic capacities of molecular sensors of the unfolded protein response to sense alternate forms of endoplasmic reticulum stress. *Mol Biol Cell* 17:3095–3107.
13. Yoshida H, et al. (2000) ATF6 activated by proteolysis binds in the presence of NF-Y (CBF) directly to the cis-acting element responsible for the mammalian unfolded protein response. *Mol Cell Biol* 20:6755–6767.
14. Johnson AE, van Waes MA (1999) The translocon: A dynamic gateway at the ER membrane. *Annu Rev Cell Dev Biol* 15:799–842.

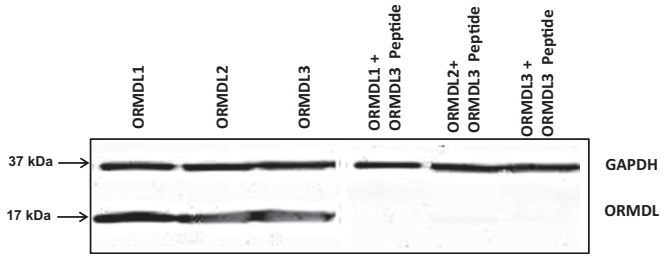

Fig. S1. Anti-ORMDL Ab. A Western blot of cell lysates transfected with ORMDL-1, ORMDL-2, or ORMDL3 was probed with a polyclonal rabbit anti-mouse ORMDL Ab. GAPDH is used as control. Lanes 1–3 demonstrates that the anti–ORMDL3 Ab detects ORMDL-1, ORMDL-2, and ORMDL3. Lanes 4–6 demonstrates that preincubation of the anti-ORMDL Ab with the 34-aa ORMDL3 peptide sequence (used to immunize rabbits) blocks binding of the ORMDL Ab to ORMDL-1, ORMDL-2, and ORMDL3.

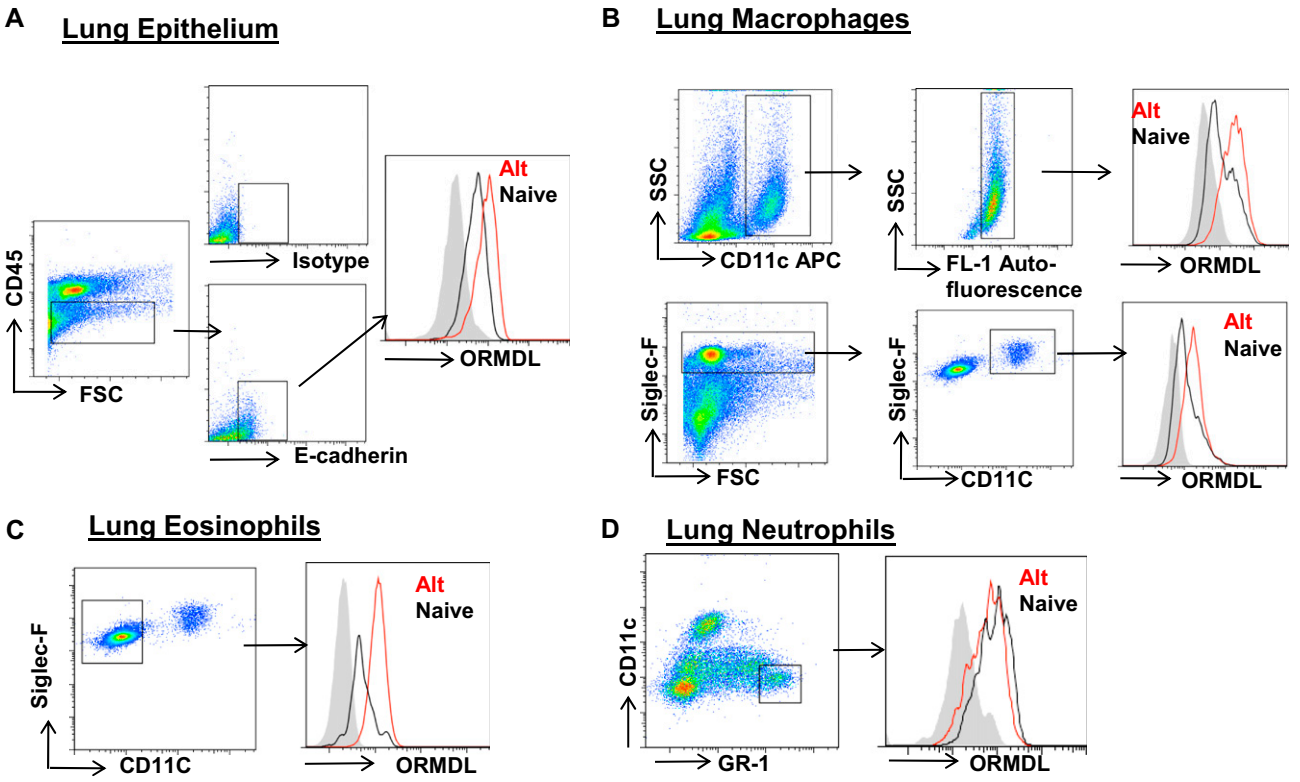

Fig. S2. ORMDL expression is induced in lung epithelial cells, macrophages, and eosinophils after allergen challenge as assessed by FACS. WT mice were challenged with *Alternaria* and lung single cell suspensions were stained and analyzed for intracellular ORMDL expression by FACS and compared with lung cells from naïve unchallenged mice. (*A*) Lung CD45-negative cells were gated (*Left*) and E-cadherin positive cells (*Center Lower*) assessed for level of ORMDL expression (*Right*). Isotype for E-cadherin shown (*Center Upper*). (*B*) Lung macrophages were identified as CD45-positive CD11c-positive autoflourescent cells (*Upper*) or CD45-positive Siglec-F–positive CD11c-positive cells (*Lower*) and ORMDL expression shown (*Right*). (*C*) Lung eosinophils were identified as Siglec-F–positive CD11c-negative cells (*Left*; gated on CD45+ Siglec-F–positive cells) and ORMDL expression shown (*Right*). (*D*) Lung neutrophils were identified as CD11c-negative GR-1–positive cells (*Left*; gated on CD45-positive cells) and ORMDL expression assessed (*Right*). Histogram of stained cells from *Alternaria*-challenged mice shown as red line, and cells from naïve mice shown as black line. Isotype staining in gray. FACS results shown are from one of two experiments of pooled lung cells from at least two mice per group. FACS results shown are from one of two experiments of pooled lung cells from at least two mice per group.

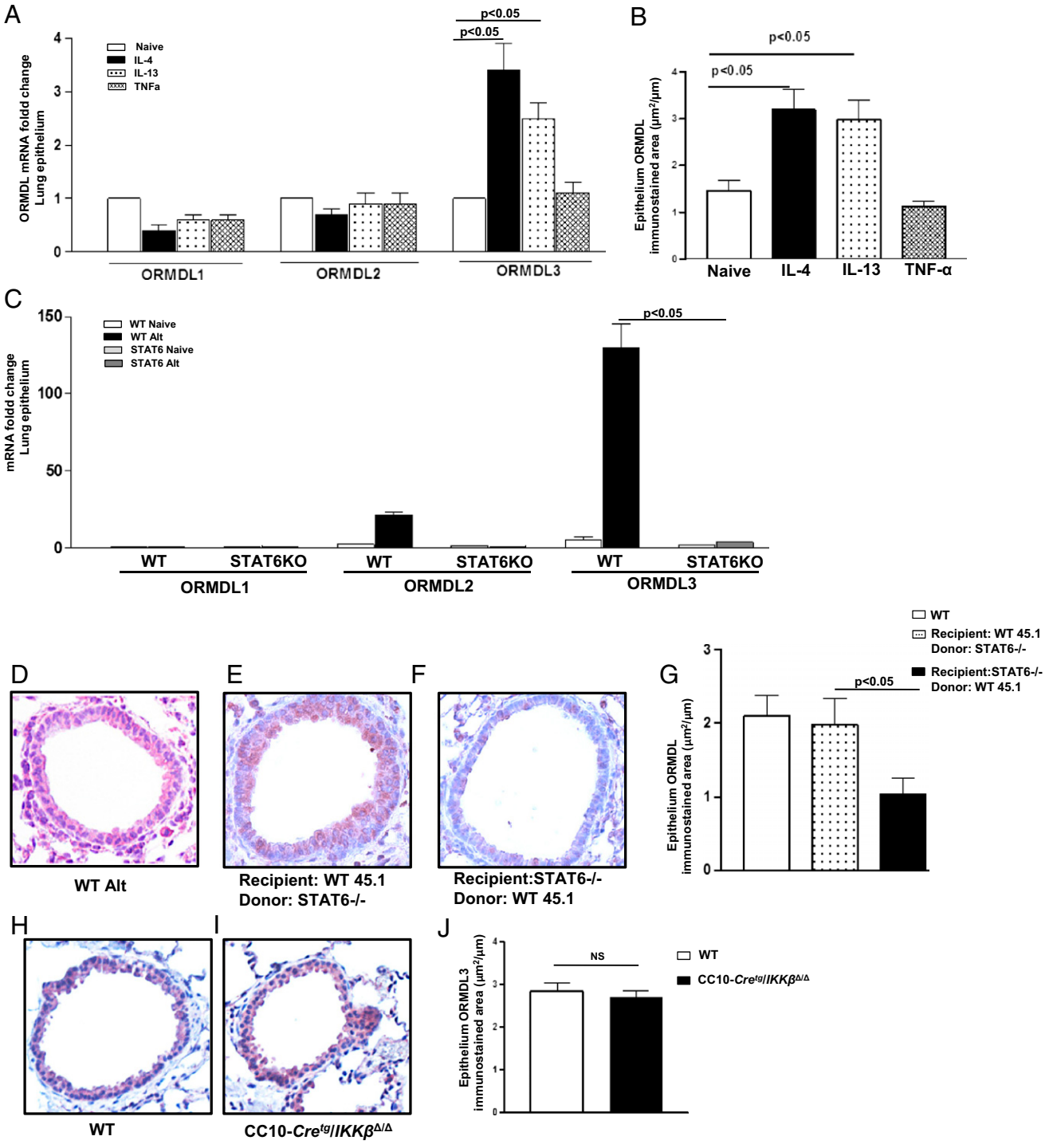

Fig. S3. Induction of ORMDL3 expression in airway epithelium depends on STAT-6 and not NF-κB. (*A*) Bronchial airway epithelial cells obtained from WT mice challenged intranasally with either IL-4, IL-13, or TNFα were processed for qPCR. IL-4 ($P < 0.05$) and IL-13 ($P < 0.05$), but not TNFα, induced a significant increase in levels of ORMDL3 mRNA. IL-4, IL-13, or TNFα did not induce ORMDL-1 or ORMDL-2 mRNA. Results are from two separate experiments with four mice per group. (*B*) Immunohistochemistry and image analysis was performed with an anti-ORMDL Ab on lungs from WT mice challenged intranasally with IL-4, IL-13, or TNFα. Results are expressed as area of ORMDL immunostaining per micrometer length of basement membrane of bronchioles, 150–200 μm of internal diameter. (*C*) WT and STAT-6 deficient mice were challenged with *Alternaria*. RNA was extracted from bronchial brushing epithelial cells. qPCR for ORMDL-1, ORMDL-2, and ORMDL3 was normalized to the housekeeping gene GAPDH. WT *Alternaria* vs. STAT-6 KO *Alternaria* (ORMDL3, $P < 0.05$; ORMDL-2, $P < 0.05$; ORMDL-1, P = ns). Results are from two separate experiments with four mice per group. (*D*–*G*) WT or STAT6$^{-/-}$ mice were irradiated and injected i.v. with WT or STAT6$^{-/-}$ bone marrow and challenged once with *Alternaria* allergen 6 wk later. *Alternaria* challenge induces Th2 cytokines and lung eosinophilia (25). WT mice (*D*) and STAT-6 chimeric mice (*E*) (with WT lung cells and STAT-6 KO bone marrow) express significant levels of ORMDL in airway epithelium after *Alternaria* allergen challenge as assessed by IHC. (*F* and *G*) In contrast, STAT 6 chimeric mice (with WT bone marrow and STAT-6 KO lung cells) do not express ORMDL in airway epithelium after allergen challenge with *Alternaria* ($P < 0.05$). *CC10-Cre^{tg}/Ikkβ$^{Δ/Δ}$*–deficient mice unable to activate NF-κB in airway epithelium (*I*) and littermate controls (*H*) express similar levels of ORMDL in airway epithelium after allergen challenge with OVA (*J*) (P = not significant).

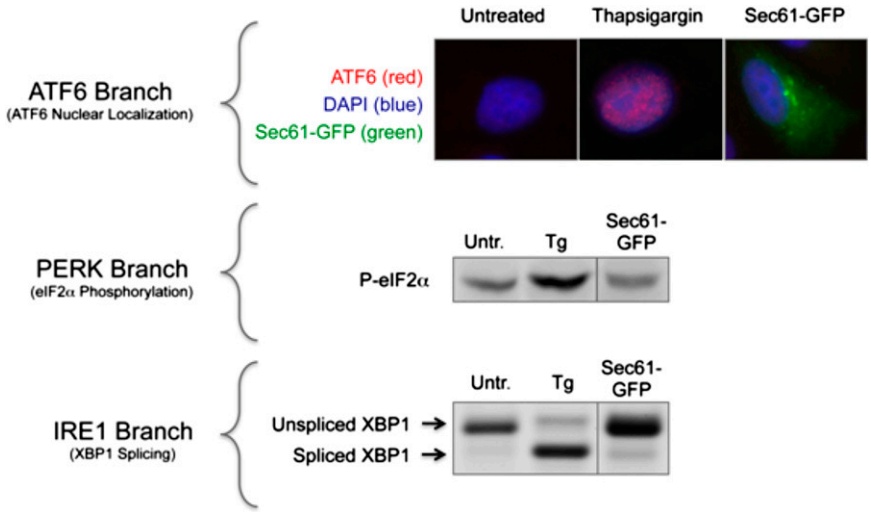

Fig. S4. Ectopic expression of an ER resident protein does not induce ATF6. Sec61α-GFP was transfected into A549 lung epithelial cells and activation of the three UPR branches determined. ATF6 activation was determined by appearance of the nuclear localized ATF6 through immunofluorescence. The color of the nuclei was altered from blue of DAPI alone (untreated) to purple with both nuclear localized ATF6 (red) and DAPI (blue) for thapsigargin (Tg) treated cells. In contrast, the nuclei of Sec61α-GFP expressed cells remained blue from DAPI, and no significant levels of the nuclear ATF6 (red) was detected, indicating that ATF6 was not activated by ectopic expression of Sec61α-GFP. PERK activation was determined by phosphorylation of eIF2α by Western blot. The level of p-eIF2α remained similar to that of untreated cells, whereas it was significantly increased upon Tg treatment. Finally, IRE1 activation was determined by splicing of XBP1 using RT/PCR of RNA isolated from either untreated, Tg treated, or Sec61α-GFP expressed cells. Positions of both unspliced and spliced XBP1 is shown.